Planar Towing and Hydroelastic Stability of Faired Underwater Cables

C. Y. Hung* and S. Nair†
Illinois Institute of Technology, Chicago, Illinois

The planar equilibrium configuration and the stability under lateral and torsional disturbances of an underwater towing cable are studied. The composite cable developed by the Boeing Company is considered as an example for numerical results. A Galerkin approximation is used to analyze the stability of the cable. Our results indicate instabilities in the form of divergence at low speeds and flutter at high speeds with stable towing for certain ranges of intermediate speeds depending on the lift-drag characteristics of the towed object.

Nomenclature

A_1 = unit vector normal to the cable in the towing plane
A_2 = unit vector normal to the towing plane
A_3 = unit vector tangential to the elastic axis
a = ratio of the distance from the hydrodynamic center to the elastic axis, to b
$a_0, a_1, a_2, b_0, b_1, c_0, c_1, c_2$ = hydrodynamic coefficients
b = half chord
$C_{L\beta}$ = lift coefficient
C_t = drag coefficient
$\boldsymbol{D}$ = damping matrix
D = drag
$\mathfrak{D}$ = differential operator, $\partial/\partial s$
D_t = drag force per unit length
$\mathfrak{D}_{vv}, \mathfrak{D}_{v\beta}, \mathfrak{D}_{\beta v}, \mathfrak{D}_{\beta\beta}$ = differential operators defined in Eq. (11)
E = Young's modulus of the constituent
EA = axial stiffness
EI_{11} = bending stiffness defined in Eq. (13)
$f_1^{(h)}, f_2^{(h)}, f_3^{(h)}$ = hydrodynamic forces per unit length
GJ = torsional stiffness
GJ_{eff} = effective torsional rigidity defined in Eq. (13)
$\boldsymbol{K}$ = stiffness matrix
L = lift
L_0 = weight in water
ℓ = length of the cable
$\boldsymbol{M}$ = mass matrix
$m_3^{(h)}$ = hydrodynamic moment about A_3
n, N = integers
Q_1, Q_2 = stiffness parameters defined in Eq. (13)
s = distance coordinate along A_3
T = cable tension
t = thickness
v = lateral perturbed displacement
$V_1, V_2, \ldots$ = Fourier components of v
W = weight per unit length under water
x', y' = trail and depth coordinates
x_1, x_2 = coordinates along A_1 and A_2
β = perturbed rotation of the cable
$\beta_1, \beta_2, \ldots$ = Fourier component of β
δ = elevator angle
θ = pitch angle
θ_g = radius of gyration about the elastic axis
θ_m, θ_n = distance from elastic axis to the center of mass, and neutral axis, respectively
λ = eigenvalue
$\text{Re}\lambda$, $\text{Im}\lambda$ = real and imaginary part of λ, respectively
κ = curvature, $-d\phi/ds$
ρ = density of water
ρ_c = density of the constituent
ϕ = angle between $-A_3$ and the vertical
ψ = eigenvector defined in Eq. (19).
$( )$ = differential operator, $\partial/\partial t$

Received July 26, 1983; revision received Feb. 14, 1984.

*Graduate Student.
†Associate Professor, Department of Mechanical and Aerospace Engineering. Member AIAA.

Introduction

DESIGN and analysis of towing cables have received considerable attention due to their applications in towing a wide variety of objects. These objects range from small underwater sensors to giant oil platforms. The development of high-speed surface craft, such as the hydrofoil, has made it feasible to increase the towing speeds of submerged sensors and marine research vehicles. To alleviate the increased drag and cable tension accompanying higher speeds, recent designs have incorporated integral fairings to achieve streamlined cable cross sections. An example of such a cable is that developed by the Boeing Company (Fig. 1). This design utilizes an NACA 63A022 section. Molded fiberglass is used for strength. A flexible hypalon rubber fairing is bonded to the strength member to provide the necessary aft contour.

As with an airplane wing, streamlined cross sections may lead to hydroelastic instabilities in the form of divergence or flutter. These instabilities may result in unnecessarily large noise levels, guidance problems, increased power requirements, and even structural failure.

This paper considers the consequences of subjecting a steady-state towing configuration to small disturbances in the form of lateral displacements and rotations. The steady-state equilibrium configuration of a cable has been the subject of a number of articles.[1-4] One of the major concerns in these studies has been the representation of the hydrodynamic loading functions. The stress-strain behavior of the cable itself does not contribute in any significant way to the equilibrium configuration. Recently, Calkins[5] has reported excellent agreement between results obtained from analysis and towing trials using the Boeing cable. Reference 5 summarizes the results of a number of studies (see references cited therein) conducted by Calkins and coworkers with a cable attached to a towed body which can be controlled in pitch, yaw, and roll. In the present study we consider the system used by Calkins[5] as an example to illustrate our results.

The stability of the equilibrium configuration has been considered by Cannon and Genin[6] and Nair and Hegemier.[7]

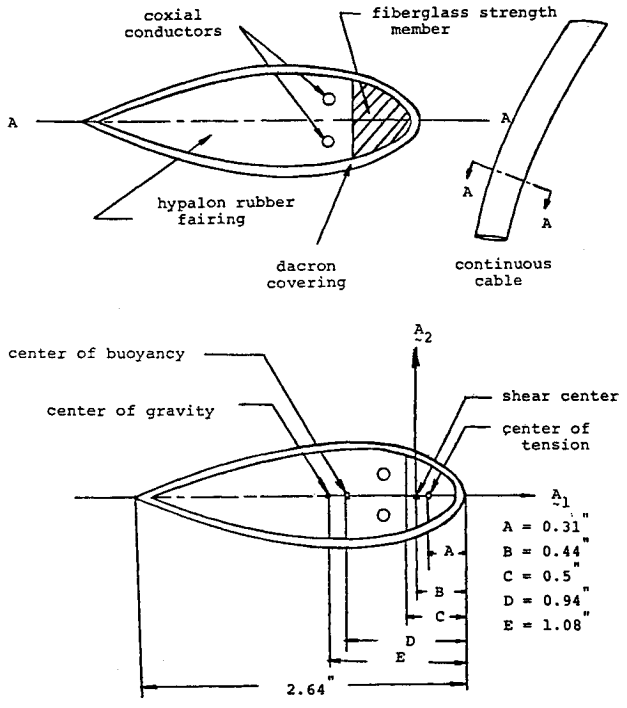

Fig. 1 Cross section of the Boeing cable.

An excellent survey of the work in hydrodynamic loading functions, equilibrium, and stability up to 1970 is given in Ref. 8. In Ref. 6 the bending stiffness of the cable has been neglected in the analysis. A system of accurate dynamic equations are developed in Ref. 7, which take into account the bending and torsional stiffness of the cable. An asymptotic solution of these equations attempted in Ref. 7 turns out to be inadequate to describe the cable behavior, as will be demonstrated in the present study.

Steady-State Towing

The steady-state, planar towing configuration of the cable is shown in Fig. 2. The distance coordinate measured from a hinged joint connecting the cable to the surface craft runs along the elastic axis (locus of shear centers) of the cable. The cable is attached through another hinged joint to the towed body at $s=\ell$. The angle between the vertical and the tangent to the cable is denoted by ϕ. The tension applied to the cable at $s=\ell$ can be varied by controlling the elevator angle δ of the towed body. Unit vectors A_3 tangential to the cable, A_1 in the plane of towing, and A_2 normal to this plane are used with coordinates s, x_1, and x_2, respectively. The tangential and normal equilibrium equations are given by

$$T' + f_3^{(h)} + f_3^{(g)} = 0 \tag{1}$$

$$T\phi' + f_1^{(h)} + f_1^{(g)} = 0 \tag{2}$$

where T is the cable tension and the f terms represent external forces. Superscripts g and h represent gravitational and hydrodynamic forces. The buoyancy effects are included in the $f^{(g)}$ terms. A prime indicates differentiation with respect to s. With w representing the weight per unit length of the cable in water,

$$f_1^{(g)} = -w\sin\phi, \qquad f_3^{(g)} = w\cos\phi \tag{3}$$

The hydrodynamic loading functions for the Boeing cable are given in Ref. 5 as

$$f_1^{(h)} = [1.04\cos\phi - 0.0334\cos 3\phi - 0.0083\cos 5\phi]D_t$$

$$f_3^{(h)} = [0.6332\sin\phi - 0.1246\sin 3\phi + 0.0132\sin 5\phi]D_t \tag{4}$$

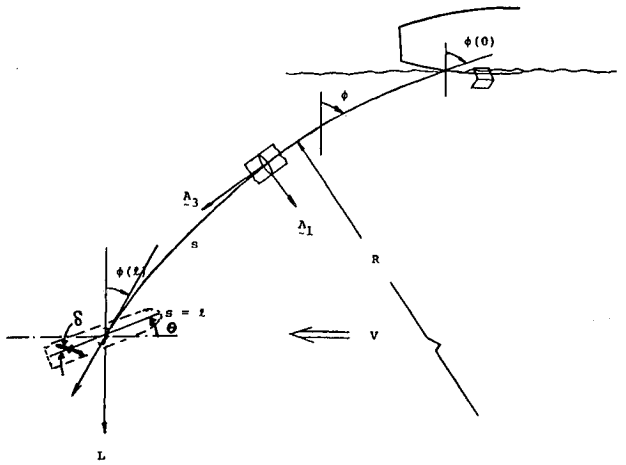

Fig. 2 Steady-state towing configuration.

where D_t, the drag force per unit length of the cable when $\phi=0$, is given by

$$D_t = \tfrac{1}{2}\rho t C_t V^2 \tag{5}$$

where ρ is the density of water, t the thickness of the cable, V the towing speed, and C_t the drag coefficient of the cable given in Ref. 5 as a function of the flow Reynolds number.

The boundary conditions required for the solution of Eqs. (1) and (2) are given by

$$T(\ell) = \sqrt{D^2 + L^2}, \qquad \phi(\ell) = \tan^{-1}(D/L) \tag{6}$$

where D is the drag and L the downward lift on the towed body.

Following the procedure used by Calkins,[5] the pitch angle θ of the towed body is set at a fixed value by controlling the elevator angle δ for different towing speeds.

The relation between δ and θ given in Ref. 5 can be expressed as

$$\delta = c_0 + c_1\theta - c_2/V^2 \tag{7}$$

where c_0, c_1, and c_2 are the hydrodynamic constants for the towed body.

The drag and lift forces on the towed body can be expressed as

$$D = (b_0 + b_1 0 + b_1\theta)V^2$$

$$L = L_0 + (a_0 + a_1\theta + a_2\delta)V^2 \tag{8}$$

using the data given in Ref. 5, where L_0 is the weight of the towed body in water and a and b are constants.

Parameters T and ϕ describing the equilibrium configuration of the cable now can be obtained using Eqs. (1) and (2) for any given pitch angle θ.

Dynamic Stability

The dynamic equations describing the lateral displacement v and rotation β of the cable when subjected to small perturbations from the equilibrium state are derived in Ref. 7. These are:

$$\mathfrak{D}_{vv}v + \mathfrak{D}_{v\beta}\beta - f_2^{(h)} = 0 \tag{9}$$

$$\mathfrak{D}_{\beta v}v + \mathfrak{D}_{\beta\beta}\beta - m_3^{(h)} = 0 \tag{10}$$

where the differential operators $\mathfrak{D}_{vv}$, $\mathfrak{D}_{v\beta}$, $\mathfrak{D}_{\beta v}$, and $\mathfrak{D}_{\beta\beta}$ are

$$\mathfrak{D}_{vv}=\overline{EI}_{22}\mathfrak{D}^4+[(\overline{EI}_{11}-\overline{EA}\,\theta_n^2-\overline{GJ}_{\text{eff}})\kappa-T\theta_n]\times(\kappa\mathfrak{D}^2+\kappa'\mathfrak{D})+[2(\overline{EI}_{11}-2\overline{EA}\theta_n^2-\overline{GJ})\kappa'-Q_1\times(T'\kappa+T\kappa')+2Q_2\kappa\kappa'-2\theta_nT']\kappa\mathfrak{D}-T\mathfrak{D}^2+m\partial^2/\partial t^2$$

$$\mathfrak{D}_{v\beta}=-\overline{EI}_{22}(\kappa\mathfrak{D}^2+2\kappa'\mathfrak{D}+\kappa'')+[(\overline{EI}_{11}-\overline{EA}\theta_n^2-\overline{GJ}_{\text{eff}})\kappa-T\theta_n^2]\mathfrak{D}^2+[(2\overline{EI}_{11}-2\overline{EA}\theta_n^2-\overline{GJ})\kappa'-Q_1(T'\kappa+T\kappa')+2Q_2\kappa\kappa'-2\theta_nT']\mathfrak{D}+T\kappa+m\theta_m\partial^2/\partial t^2$$

$$\mathfrak{D}_{\beta v}=-\overline{GJ}_{\text{eff}}(\kappa\mathfrak{D}^2+\kappa'\mathfrak{D})-[(\overline{EI}_{22}-\overline{EI}_{11}+\overline{EA}\theta_n^2)+T\theta_n]\times\mathfrak{D}^2+m\theta_m\partial^2/\partial t^2$$

$$\mathfrak{D}_{\beta\beta}=-\overline{GJ}_{\text{eff}}\mathfrak{D}^2+[(\overline{EI}_{22}-\overline{EI}_{11}+\overline{EA}\theta_n^2)+T\theta_n]+m\theta_g^2\partial^2/\partial t^2 \tag{11}$$

The hydrodynamic force $f_2^{(h)}$ and moment $m_3^{(h)}$ are taken in accordance with the velocity component strip theory[9] for hydrofoils oscillating in a simple harmonic motion. For low-frequency motions these can be taken as

$$f_2^{(h)}=C_{L\beta}\rho bV_n[V_n(\beta-\tan\phi v')-\dot{v}+(\tfrac{1}{2}-a)b(\dot{\beta}+V_n\tan\phi\beta'')]+\tfrac{1}{2}C_{L\beta}\rho b^2[V_n(\dot{\beta}-\tan\phi v'')-\ddot{v}-ab(\ddot{\beta}+V_n\tan\phi\beta'')]$$

$$m_3^{(h)}=C_{L\beta}\rho b^2V_n(a+\tfrac{1}{2})[V_n(\beta-\tan v')-\dot{v}+(\tfrac{1}{2}-a)b(\dot{\beta}+V_n\tan\phi\beta')]+\tfrac{1}{2}C_{L\beta}\rho b^2[V_n(\overline{a-\tfrac{1}{2}}\dot{\beta}-a\tan\phi v'')-a\ddot{v}-\tfrac{1}{2}V_n^2\tan\phi\beta'-(\tfrac{1}{8}+a^2)b(\ddot{\beta}+V_n\tan\phi\beta'')] \tag{12}$$

In Eqs. (11) and (12), the following definitions have been used:

$$\overline{EI}_{ij}=\int Ex_ix_j\,dA$$

$$\overline{EA}=\int E\,dA$$

$$m=\int\rho_c\,dA$$

$$\overline{GJ}_{\text{eff}}=(\overline{GJ}+Q_1T-Q_2\kappa$$

$$Q_1=(\overline{EI}_{11}+\overline{EI}_{22})/\overline{EA}$$

$$Q_2=\overline{EA}\,Q_1\theta_n-\int E(x_1^2+x_2^2)x_1\,dA$$

$$\theta_n=\int Ex_1\,dA/\overline{EA}$$

$$\theta_m=\int\rho_cx_1\,dA/m$$

$$\theta_g^2=\int\rho_c(x_1^2+x_2^2)\,dA/m \tag{13}$$

The homogeneous system of Eqs. (9) and (10) must be solved with the boundary conditions

$$v=0,\quad \beta=0\quad\text{at}\quad s=0\text{ and at }s=\ell \tag{14}$$

The boundary conditions at $s=\ell$ are based on the assumption that the inertia of the towed body is large enough to prevent any lateral motion or rotation at the lower terminus of the cable.

The nonconstant coefficients in the system of equations depend on the steady-state configuration through the variables T, ϕ, and their derivatives.

Solution of these equations are sought in the form

$$v=e^{\lambda t}\sum_{n=1}^{N}v_n\sin\frac{n\pi s}{\ell}$$

$$\beta=e^{\lambda t}\sum_{n=1}^{N}\beta_n\sin\frac{n\pi s}{\ell} \tag{15}$$

where the eigenvalues λ and the eigenvectors (v_n, β_n) are to be determined. Our approximate solution (15) will yield $4N$ eigenvalues. The onset of instability is indicated by the condition

$$\text{Re}\lambda=0 \tag{16}$$

Unstable motion of the cable can be classified as: divergence when

$$\text{Re}\lambda>0,\qquad \text{Im}\lambda=0$$

and flutter when

$$\text{Re}\lambda>0,\qquad \text{Im}\lambda\neq0 \tag{17}$$

Using the Galerkin method, the system of Eqs. (9) and (10) is converted to the matrix system

$$[M\lambda^2+D\lambda+K]\{\psi\}=0 \tag{18}$$

where

$$\{\psi\}^T=[v_1,\beta_1,v_2,\beta_2,\ldots,v_N,\beta_N] \tag{19}$$

The eigenvalues and eigenvectors of the above system can be obtained for different tow speeds and pitch angles of the towed body.

Numerical Results

The Boeing cable is considered to illustrate the stability analysis discussed herein. Since Calkins[5] has obtained trial data on this cable, it is also possible to compare the steady-state results herein with those in Ref. 5. Numerical values for the parameters describing the cable are listed in Table 1. The hydrodynamic data pertaining to the towed body are listed in Table 2. These data are based on the properties of the cable and towed body presented in Ref. 5. A computer program was written to calculate the steady-state configuration and to implement the Galerkin scheme. The differential equations (1) and (2) are integrated numerically using Adam's four-point scheme. The cable length was assumed to be 121.92m (400 ft), as in Ref. 5. The x' and y' coordinates of the cable measured at the points $s=\ell$, the maximum tension $T(0)$, and the angle $\phi(0)$ are given in Table 3 as functions of the number of integration intervals used. These values indicate that $M=50$ gives sufficient accuracy; in all subsequent calculations M was taken as 50.

In Table 4, a comparison of our steady-state towing results with Calkins[5] trial data and numerical simulation is given. Our calculations, as well as those in Ref. 5, underestimate the maximum cable tension. This could possibly be due to a small permanent twist in the cable used for the trials, as noted by Calkins.[5] There is fair agreement between all other steady-state parameters and the differences between our results and the calculated values in Ref. 5 are due to numerical errors. The cable configurations for different towing speeds are

Table 1 Cable parameters

$a = -0.664$	$b = 0.0335$ m (0.11 ft)
$\overline{EA_{11}} = 140.84$ Nm^2 (340.84 lb ft^2)	$\overline{EI_{22}} = 32.55$ Nm^2 (78.77 lb ft^2)
$\overline{EA} = 6.36 \times 10^6$ N (1.43×10^6 lb)	$\overline{GJ} = 27.81$ Nm^2 (67.31 lb ft^2)
$m = 1.05$ kg/m (0.707 lbm/ft)	$w = 0.40$ kg/m (0.269 lb/ft)
$t = 0.0148$ m (0.58 in.)	$C_{L\beta} = 6.8238$
$\theta_m = -0.126$ m (-0.414 ft)	$\theta_n = 0.00335$ m (0.011 ft)
$\theta_g = 0.0695$ m (0.228 ft)	$T_{\text{working}} = 44{,}480$ N (10,000 lb)

Table 2 Towed body parameters

L_0	= 1984 N (446 lb)
a_0	= 73.74 kg/m (1.54 slugs/ft)
a_1	= -546.3 kg/m rad (-11.41 slugs/ft rad)
a_2	= 61.29 kg/m rad (1.28 slugs/ft rad)
b_1	= -17.24 kg/m (-0.36 slugs/ft)
b_2	= -188.6 kg/m rad (-3.94 slugs/ft rad)
c_0	= -0.153 rad
c_1	= 3.967
c_2	= 2.4368 m^2 rad/s^2 (26.23 ft^2 rad/s^2)

Table 3 Convergence of numerical integration for $V = 20.85$ m/s (40.5 knots) at $\theta = 0.7$ deg

M	$T(0)$, lb	$\phi(0)$, deg	$x'(\ell)$, ft	$y'(\ell)$, ft
25	9036.54	59.48	258.52	293.19
50	9040.00	59.51	258.12	293.35
100	9040.00	59.51	257.95	293.34
200	9040.00	59.51	257.91	293.34

Table 4 Comparison with experimental and previous numerical data,[5] when $V = 20.85$ m/s (40.5 knots) and $\delta = -9.7$ deg

	Trial data[5]	Numerical[5]	Present[5]
Upper tension, lb	10163.0	9550.0	9143.0
Lower tension, lb	7950.0	7370.0	7006.0
Upper angle, $\phi(0)$, deg	53.4	54.0	56.6
Lower angle, $\phi(\ell)$, deg	14.0	16.5	13.7
Body depth, ft	305.0	296.0	307.0
Body pitch, deg	0.5	-0.3	-0.15

Table 5 Amplitude and phase angles of the modes at a pitch angle, $\theta = -3$ deg

Speed, knots	Transition	Amplitude	Phase angle, deg
32	Divergence to stable	$v_1 = 0.6979$ in.	180
		$v_2 = 1.0000$ in.	0
		$\beta_1 = 0.1897$ deg/in.	180
		$\beta_2 = 0.6241$ deg/in.	0
84	Stable to flutter	$v_1 = 0.6770$ in.	-80.1
		$v_2 = 1.0000$ in.	0
		$\beta_1 = 0.3416$ deg/in.	0
		$\beta_2 = 0.6776$ deg/in.	84.67

shown in Fig. 3 when the towed body is at a pitch angle of 0 deg. When the towing speed is above 50 knots there is very little change in the cable configuration. However, as shown in Fig. 4, the cable tension increases almost proportional to the square of the velocity.

In the Galerkin approximation all of the integrations involving the nonconstant coefficients and the basis functions $\sin(n\pi s/\ell)$ were also carried out numerically. A one-term approximation ($N = 1$) for the eigenfunctions turns out to be inadequate since the first mode of instability has a large antisymmetric $(\sin 2\pi s/\ell)$ component. Typical divergence and flutter modes obtained using a two-term approximation,

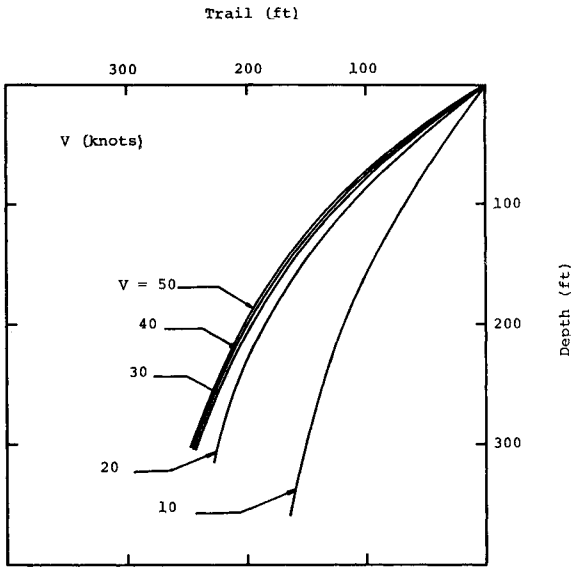

Fig. 3 Cable configurations at different speeds.

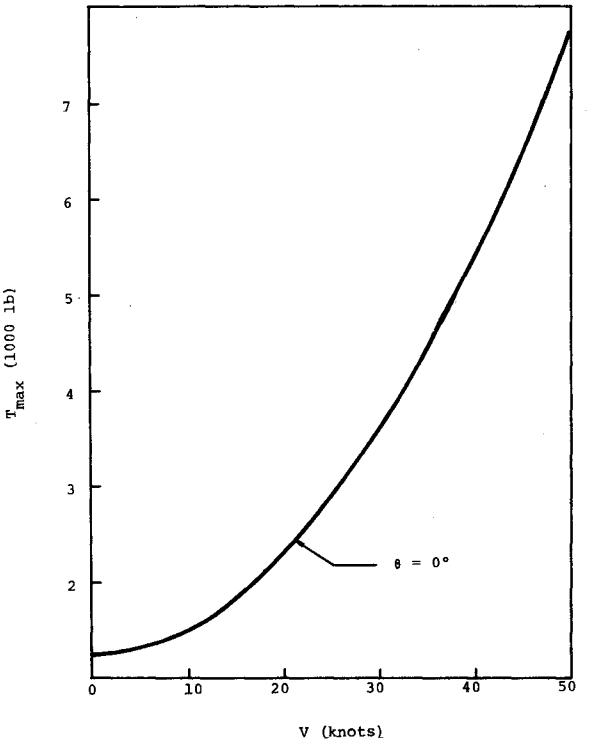

Fig. 4 Maximum cable tension as function of speed.

shown in Table 5, confirm this observation. The results presented in Table 5 correspond to a pitch angle of -3 deg.

Critical speeds obtained for different pitch angles θ using the two-term approximation are shown in Fig. 5. Here, for a given value of the pitch angle, solid lines indicate the range of towing speeds and the elevator angles for stable towing. The dotted lines shown as a continuation of the solid lines indicate instability in the form of divergence in the low-speed regime and flutter in the high-speed regime. The horizontal line at $\delta = -25$ deg shows a constraint on the maximum attainable elevator angle for the towed body considered by Calkins.[5] In the same diagram a vertical curve at about 70 knots shows the limit load in tension allowed for the Boeing cable. Increased nose-down pitch angles increase the downward lift on the towed body which in turn increases the cable tension. The divergence speed can be seen to be lower in these cases. The terms which appear to be small from an asymptotic con-

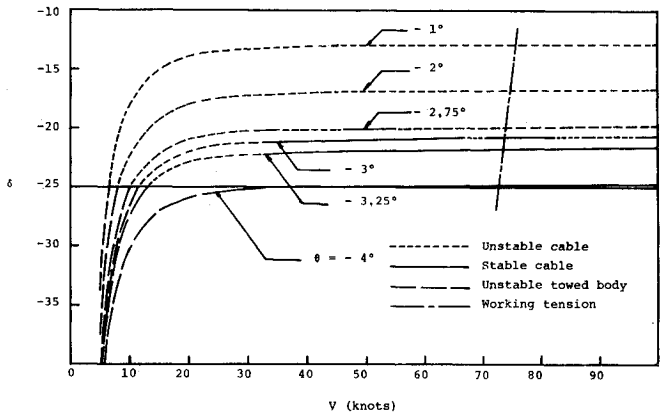

Fig. 5 Stable and unstable regime in the V-δ plane.

Table 6 Eigenvalues of Eq. (18) when $\theta = -3$ deg

$V = 31$ knots	$V = 67$ knots
0.66	$-0.027 \pm i0.57$
-0.73	$-0.009 \pm i1.17$
$-0.03 \pm i1.28$	$-774 \pm i1206$
$-357 \pm i556$	$-918 \pm i1417$
$-425 \pm i679$	

sideration in Ref. 7 are found to alter the transition speeds in a significant way.

The eigenvalues of Eq. (18) are given in Table 6. These numbers show four roots corresponding to highly damped, high-frequency oscillations and the remaining four correspond to low-frequency oscillations. One of these low-frequency modes eventually participates in the transition from stable to unstable motion of the cable. As expected, all of the results presented herein indicate that the mode of instability is divergence at low speeds and flutter at high speeds. The lower cable tension is responsible for these low-speed instabilities.

Conclusion

The linear stability of a steady-state planar towing cable is studied using the Galerkin approximation. The results show instability in the form of divergence at low speeds and in the form of flutter at high speeds. However, there is an intermediate range where stable motion is possible. The computer program developed for this study is capable of varying the cable length and the elastic and hydrodynamic parameters of the cable. The Galerkin scheme used in the numerical example needs modification to include higher order harmonics. Considering the smooth behavior of the non-constant coeffieints T and κ (shown in Figs. 3 and 4) entering the governing equations, one could expect negligible contribution due to higher harmonics. The present approximate transition speeds already indicate the characteristics of cable instability.

Acknowledgments

This paper is based on the MS Thesis submitted by the first author to the School of Advanced Studies of the Illinois Institute of Technology, Chicago. The computational facilities and computer time provided by IIT are gratefully acknowledged.

References

[1] Pode, L., "Tables for Computing the Equilibrium Configuration of a Flexible Cable in a Uniform Stream," David Taylor Model Basin, Washington, D. C., Rept. 687, March 1951.

[2] Genin, J. and Cannon, T. C., "Equilibrium Configuration and Tensions of a Flexible Cable in a Uniform Field," *Journal of Aircraft,* Vol. 4, May-June 1967, pp. 200-202.

[3] Schram, J. W. and Reyle, S. P., "A Three Dimensional Dynamic Analysis of a Towed System," *Journal of Hydronautics,* Vol. 2, Oct. 1968, pp. 213-220.

[4] Calkins, D. E., "Faired Towline Hydrodynamics," *Journal of Hydronautics*, Vol. 4, July 1970, pp. 113-119.

[5] Calkins D. E., "Hydrodynamic Analysis of a High-Speed Marine Towed System," Journal of Hydronautics, Vol. 13, Jan. 1979, pp. 10-19.

[6] Cannon, T. C. and Genin, J., "Dynamic Behavior of Material Damped Flexible Towed Cable," *Aeronautical Quarterly,* Vol. 23, May 1972, pp. 109-120.

[7] Nair, S. and Hegemier, G., "Stability of Faired Underwater Towing Cables," *Journal of Hydronautics*, Vol. 13, Jan. 1979, pp. 20-27.

[8] Casarella, M. J., and Parsons, M., "Cable Systems under Hydrodynamic Loading," *MTS Journal,* Vol. 4, July-Aug. 1970.

[9] Bisplinghoff, R. L., Ashley, H., and Halfman, R. L., *Aeroelasticity,* Addison-Wesley, Cambridge, Mass., 1957.